ANALYTICAL STUDY ON THERMAL STRESS OF AUTOCLAVED AERATED CONCRETE SHEAR WALLS

YAOHUI MA[1], DEZHI ZHAO[2] *, LIN CHI[2]*, ZHENG WANG[2], YAN YAO[3], SHUANG LU[2,3]

[1] Heilongjiang institute of hydraulic science, Harbin, Heilongjiang, China
[2] Department of Civil Engineering, Harbin Institute of Technology, Harbin, Heilongjiang, China
[3] China Building Materials Academy, Beijing, China

In this numerical study, finite element method (FEM) is employed to demonstrate temperature and stress simulations of autoclaved aerated concrete (AAC) shear walls in different seasons by using ANSYS software. Structural behavior simulation is conducted by a good combination of comprehensive material properties and reasonable models. Calculation results show that, compared with the ordinary mortar (OM), the insulation mortar (IM) can effectively reduce f temperature variation in AAC matrix layer by 1.668℃ in summer and 5.315℃ in winter, which indicates a better performance on heat insulation. In terms of thermal stress, IM layer would withstand a greater stress in all cases, but it could lower the maximum stress in AAC layer and interface stress by almost 50% in winter compared with wall structures with OM. As for temperature deformation, a 17% reduction in winter and a 30% reduction in summer are observed in AAC matrix layer coated with IM.

Keywords: *FEM, AAC shear walls, thermal stress, temperature deformation*

1. Introduction

At present, energy consumed in construction industry almost takes up 40% of total energy consumption in China. Hence, in terms of energy conservation and environmental protection, improving thermal insulation performance of the external walls is well recommended.

Autoclaved Aerated Concrete (AAC) is one of the most effective wall materials but the rarely elective external insulation system might meet the requirement of 65% building energy saving policy in China [1]. AAC self-insulation system is widely used in favor of light weight, heat preservation, excellent seismic performance and suitable strength. The most attractive point of AAC is its relative low thermal conductivity compared with the ordinary concrete. Researchers have extensively studied the comprehensive properties of AAC, such as microstructure [2,3], density [4,5], strength [6-9], shrinkage [10-12] and so on.

In practice, the performance of the AAC shear walls is inherently influenced by various environmental loads including such as temperature, airflow and moisture. Among these factors, temperature variation plays a crucial role which may influence the thermal stress distribution within the wall structure. Especially in hot summer and cold winter, considerable thermal stress will be caused by temperature difference between the interior and exterior walls which may cause inconsistent deformation between the AAC walls and the surface mortar, resulting in surface splitting and durability deterioration to some extent.

However, reliable experimental data are difficult to obtain, as the experiments are susceptible to test methods and conditions, both leading to precision decrease. Therefore, numerical simulation is applied to evaluate the properties of building structures. For example, FLUENT software is adopted to explore the effect of enclosure configurations with the same void volume fraction on equivalent thermal conductivity [13,14]. Du and Shi [15] have analyzed the temperature distribution law of the precast box girders by the finite element numerical simulation method. Larbi [16] has studied the heat transfer coefficients of three wall structures by using 2D numerical calculations. It is concluded that the static models can present the thermal properties of walls to some extent. Asan [17] has optimized the intermediate position of the insulation layer of specific wall structure according to the Crank-Nicolson equation. Calculation results suggest that two separate insulation layers located

* Autor corespondent/*Corresponding author*,
E-mail: 244722305@qq.com
* Autor corespondent/*Corresponding author*,
E-mail: 984437353@qq.com

both in the middle and outside the exterior wall will be better. To avoid moisture condensation, Kočí *et al.*[18] have modified the AAC wall structure with extra insulation layer that composed of different materials and then analyzed the moisture transition across the wall structure by conducting numerical calculations.

Overall, the numerical simulation is successfully applied into thermal calculation and some satisfactory results are obtained. In this paper, ANSYS software [19] is used to access the temperature field, thermal stress and deformation of AAC shear walls, aiming to solve some practical issues, such as interlayer separations and cracks.

2. Research Significance

The application of FEM has provided a relative reliable method to analyze the stress and deformation of AAC shear walls. In practice, cracking usually emerging on the surface layer of the mortar,followed by a severe interfacial separation from the AAC layer. Therefore, there is a need assessing the potential deformation of exterior walls to avoid the undesirable failure. Before the numerical analysis, a series of experiments about the properties of AAC and different mortars are conducted.

In this paper, appropriate FEM model is established to analyze the stress field and the deformation in the AAC shear walls that are coated by two different surface mortars: ordinary mortar (OM) and insulation mortar (IM). Taking into account the worst-case scenario, corresponding analysis is performed to obtain the temperature field, stress field and deformation of the AAC shear walls in both hot summer and cold winter.

3. Finite Element Modeling

3.1.Mathematical model

Mathematical model is firstly established before numerical simulation. Assuming that the wall is apparent to be homogeneous and continuous, that is comprised of several closely connected material units so that the thermal resistance introduced by each interface could be ignored. According to the law of conservation of energy and Fourier's law, function of temperature (T) of spatial points (x, y, z) at any moment (t) is established as Eq. (1).

$$\rho c \frac{\partial T}{\partial t} = \frac{\partial}{\partial x}(\lambda \frac{\partial T}{\partial x}) + \frac{\partial}{\partial y}(\lambda \frac{\partial T}{\partial y}) + \frac{\partial}{\partial z}(\lambda \frac{\partial T}{\partial z}) + Q_v \quad (1)$$

Where λ represents coefficient of thermal conductivity [W/(m·K)], c represents specific heat capacity [J/(Kg·K)], ρ represents density [Kg/m^3] and Q_v represents heat discharge in per time per unit volume [W/m^3]. In this paper, the wall system is supposed to be stable heat-transfer media, thus, λ, c and ρ are all constants in the model. Meanwhile, there is no heat source inside the wall (Q_v=0).

Therefore, Eq. (1) can be simplified into following format,

$$\frac{\partial T}{\partial t} = \frac{\lambda}{\rho c}(\frac{\partial^2 T}{\partial x^2} + \frac{\partial^2 T}{\partial y^2} + \frac{\partial^2 T}{\partial z^2}) \quad (2)$$

There has been some general solution for the Eq. (2). For different heat transfer process, combined with its boundary conditions, the calculation results can be obtained.

Figure 1 has shown the typical size of the AAC shear wall commonly used in China, with 3000 mm in length, 240 mm in width, and 2000 mm in height. During the analysis, a surface mortar layer with 20 mm in thickness is attached to the exterior surface of AAC layer.

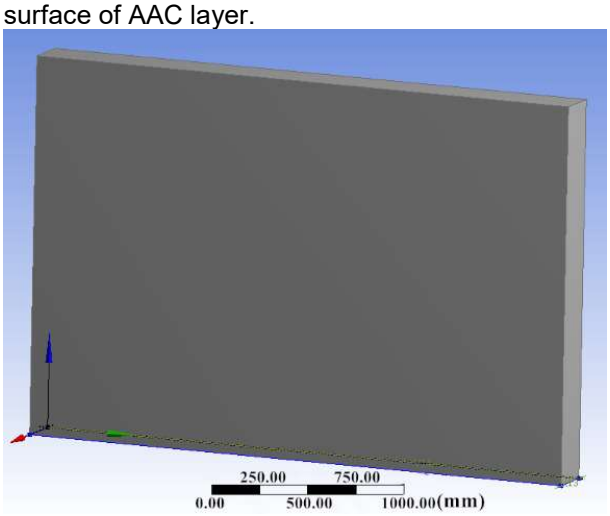

Fig.1 - Schematic diagram of geometry model.

3.2. Boundary conditions

The boundary conditions are nominated as follows.

$$x = 0 \quad h_{out}(T_{out} - T_{f_2}) = \lambda \frac{\partial T}{\partial x} \quad (3)$$

$$x = W \quad h_{in}(T_{f_1} - T_{oin}) = \lambda \frac{\partial T}{\partial x} \quad (4)$$

$$y = 0 \quad \lambda \frac{\partial T}{\partial y} = 0 \quad (5)$$

$$y = L \quad \lambda \frac{\partial T}{\partial y} = 0 \quad (6)$$

$$z = 0 \quad \lambda \frac{\partial T}{\partial z} = 0 \quad (7)$$

$$z = H \quad \lambda \frac{\partial T}{\partial z} = 0 \quad (8)$$

where L, W and H represent the length, width, and height, respectively; h_{in} and h_{out} represent convection heat transfer coefficient indoor and outdoor. The direction of the heat transfer is in the x direction. Thus, x = 0 is for outer surface and x = W is for interior surface.

Based on China standard “Code for thermal design of civil buildings” (GB 50176-2002), h_{in} and h_{out} are chosen as 8.7 W/(m^2·K) and 23.3 W/(m^2·K), respectively. However, it should be noted that h_{out} actually is not constant no matter in winter or in summer. The indoor temperature is supposed to be fixed at 18℃throughout the simulation. For outdoor temperature, they are supposed as -20℃ in winter

Table 1

The thermal physical properties using in the numerical simulation

Property	AAC	IM	OM
Thermal conductivity (W/(m·K))	0.16	0.06	0.93
Density (Kg/m^3)	500	300	1800
Thermal expansion coefficient (K^{-1})	1.0×10^{-5}	1.2×10^{-5}	1.2×10^{-5}
Elastic modulus (MPa)	2000	15000	5000
Poisson ratio	0.2	0.25	0.28

and 30℃ in summer, according to the average daytime temperature of the coldest week and hottest week in recent 5 years in Harbin China, respectively. Besides, two assumptions are made during the numerical calculation. The first one is steady-state heat transfer process assumption. Temperatures inside and outside are unchangeable, so it's a steady-state heat transfer process at any time. The other is that the thermal contact resistance between different material layers could be ignored. As uneven surface of different materials would lead to unclosed contact, there will be a temperature difference on both sides of the interface, and heat conduction will occur, such resulting in thermal contact resistance. Due to the thermal resistance takes up only a small proportion, the influence is neglected in the process of finite element simulation analysis. The thermal and physical properties of the materials employed are listed in Table 1.

3.3. Mesh generation

Considering the thermal and structural analysis, a three-dimensional hexahedral element, with 20 nodes, is used for each numerical model. Thus, 449,109 nodes and 103,968 elements will be generated totally for specific simulated wall structure.

4. FEM analysis results and discussion

In the paper, two wall structures, 240mm AAC matrix layer with a 20 mm IM layer and OM layer (WS1 and WS2), has been analyzed in both hot summer and cold winter. By theoretically varying the outdoor temperature, the thermal stress and deformation of different walls as well as the corresponded temperature field are simulated by ANSYS software.

4.1. Temperature field analysis

During the temperature field analysis, boundary conditions of y direction and z direction (width and height direction) are both considered as two adiabatic conditions. Heat transfer is simplified to appear merely in x direction (thickness direction). Figure 2 and Figure 3 show the temperature field distributed in the WS1 and WS2 in cold winter and hotsummer, respectively. As shown in Figure 2 and 3, the temperature varied gradually in the thickness directions. In winter, the surface temperatures of interior and exterior of WS1 are 15.806℃ and -19.181℃, and 15.399℃ and -19.029℃ for WS2. In summer, these temperatures are 18.693℃ and 29.741℃ for WS1, and 18.821℃ and 29.693℃ for WS2. Compared with WS2, the interior surface temperature of WS1 has a 0.407℃ increase in winter and 0.128℃ decrease in summer. Therefore, it can be concluded that WS1 has a better heat insolation performance no matter in summer or in winter.

Figure 4 presents the temperature distribution within the WS1 and WS2 in winter and summer. As shown in the Figure 4, in winter, the temperatures near the interface between AAC and mortar are -12.820℃ for WS1 and -18.542℃ for WS2. When in summer, the interface temperature are 27.733℃ and 29.693℃ for WS1 and WS2. The temperature change in AAC layer of WS1 is

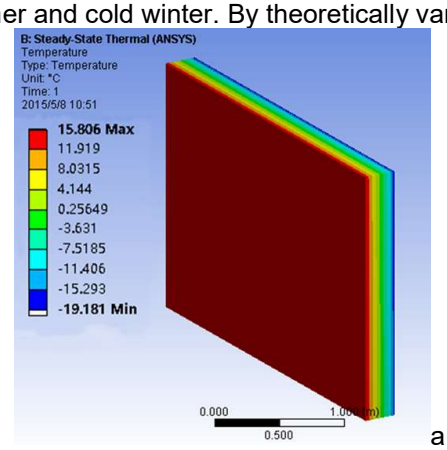

a

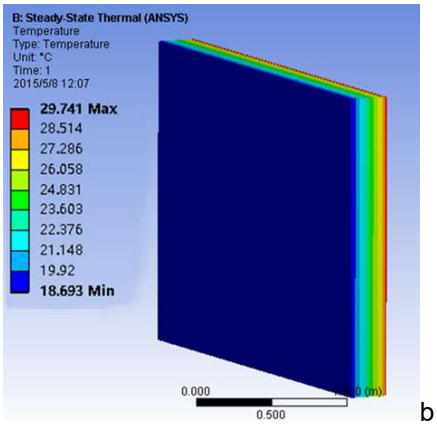

b

Fig.2 - Temperature field of WS1 in winter (a) and summer (b).

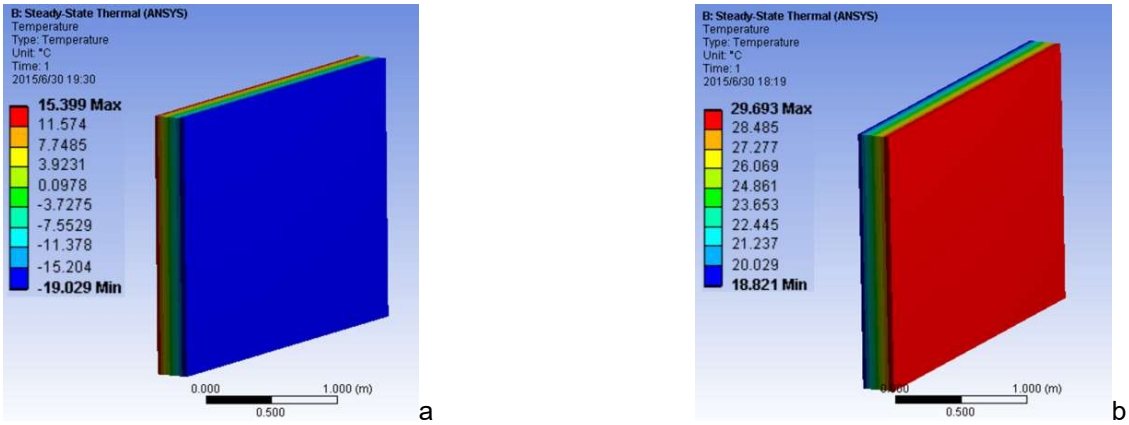

Fig.3 - Temperature field of WS2 in winter (a) and summer (b).

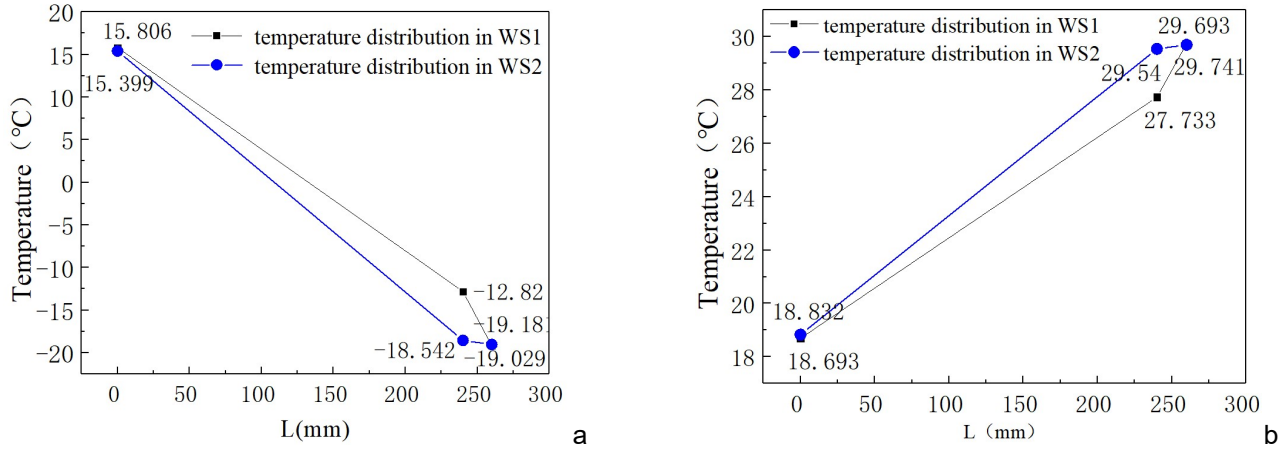

Fig.4 - Temperature distribution of WS1 and WS2 in winter (a) and summer (b).

28.626℃ in winter and 9.040℃ in summer, while that in WS2 is 33.941℃ in winter and 10.708℃ in summer, both larger than the former. It demonstrates that, when coated with IM, AAC layer experience less temperature variation. As IM has better a heat insulation performance, the protective effect of mortar on AAC layer is strengthened. That would also reduce the emergence of AAC layer cracking, thus enhancing the durability of wall structures. Besides, a larger temperature gradient also indicates a larger temperature deformation in IM layer.

4.2. Thermal stress analysis

Due to the uneven temperature change and different physical properties of AAC layer and mortar layer, thermal stress and deformation would be questionable, which might have potential negative influence on volume stability and long-term durability of the structure. In the process of stress analysis, the wall is regarded as an embedded slab.

Figure 5 and Figure 6 illustrate the thermal stress distribution within two wall systems in both winter and summer. In winter, the maximum stress of WS1 is observed on the exterior surface, reaching 17.32 MPa. The interface stress is about 1.93 MPa as shown in Figure 5 (a). For WS2 in Figure 6 (a), the stress obtained in exterior mortar layer is also the maximum value, 8.07 MPa, and the stress obtained in the interface is 3.75 MPa. Mortar layer suffers a larger thermal stress than the AAC layer, especially in WS1, as the maximum stress in WS1 is two times larger than that in WS2. However, thermal stress in AAC layer presents an opposite rule.In fact, the minimum and maximum of WS1 are 0.009 MPa and 1.93 MPa, while the data of WS2 are 0.013 MPa and 3.75 MPa, almost doubling the former. The same pattern is also observed in summer: the maximum stress is much larger in WS1 (3.03 MPa >> 1.42 MPa), while the AAC layer presents a smaller stress variation.

As mentioned, the application of IM can reduce the thermal stress introduced into the AAC layer and also diminish the stress in the interface between mortar layer and AAC layer effectively.

4.3. Temperature deformation analysis

The results of temperature deformation analysis of WS1 and WS2 in different seasons are presented in the Figure 7 and Figure 8.

In winter, the maximum structure deformation occurs in AAC layer and there is a 17% reduction in WS1 compared to WS2. While in summer, mortar layers undergo a larger deformation, which results in a lower temperature deformation in AAC layer: 9.58×10^{-6} m if maximum in WS2 and 6.74×10^{-6} m if maximum in WS1, only 70% compare with the former.

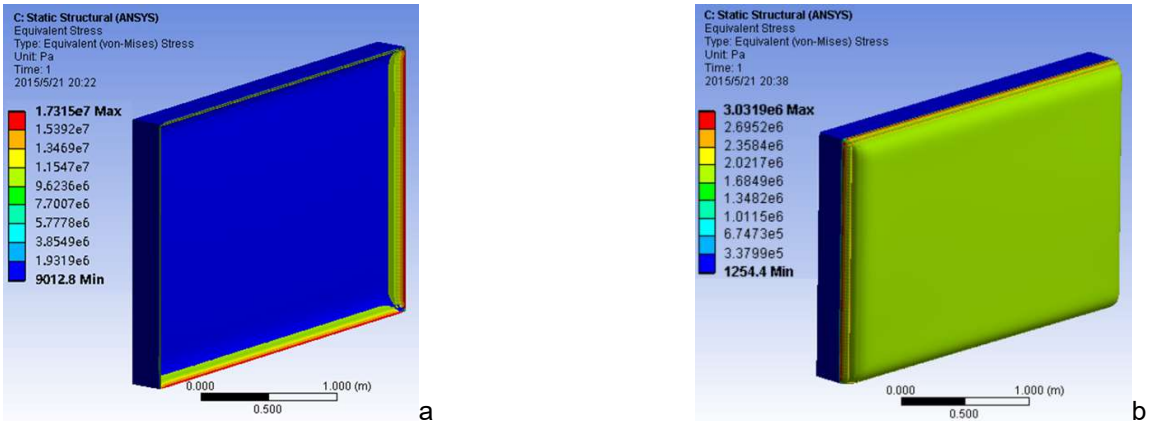

Fig.5 - Thermal stress of WS1 as embedded slab in winter (a) and summer (b).

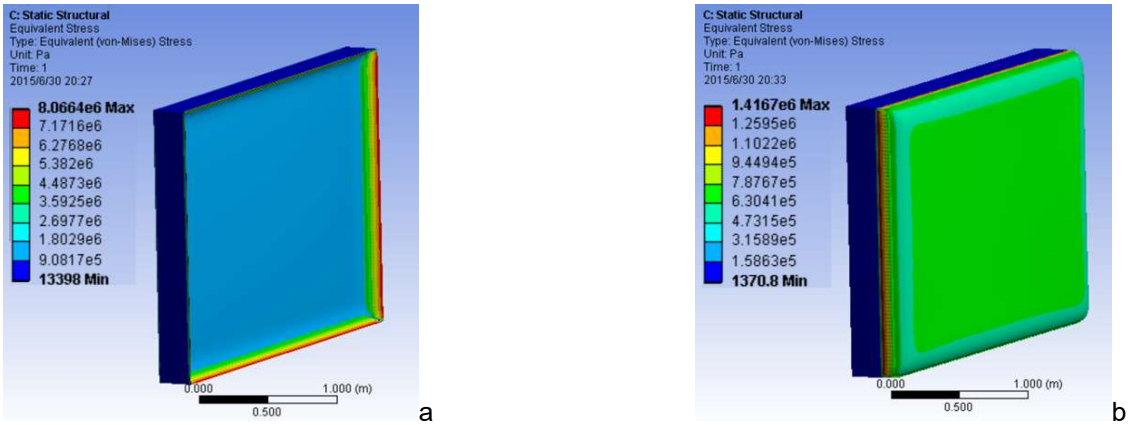

Fig.6 - Thermal stress of WS2 as embedded slab in winter (a) and summer (b)

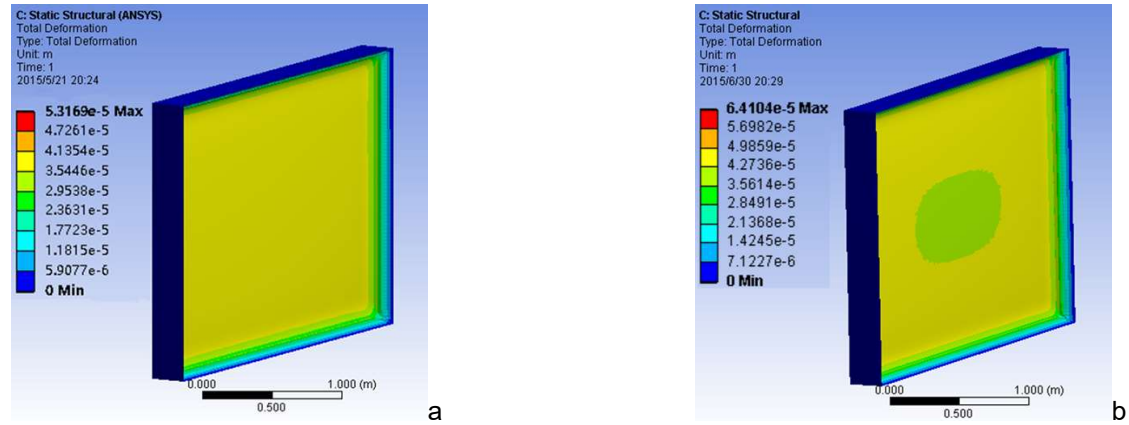

Fig.7 - Temperature deformation of WS1 as embedded slab in winter (a) and summer (b).

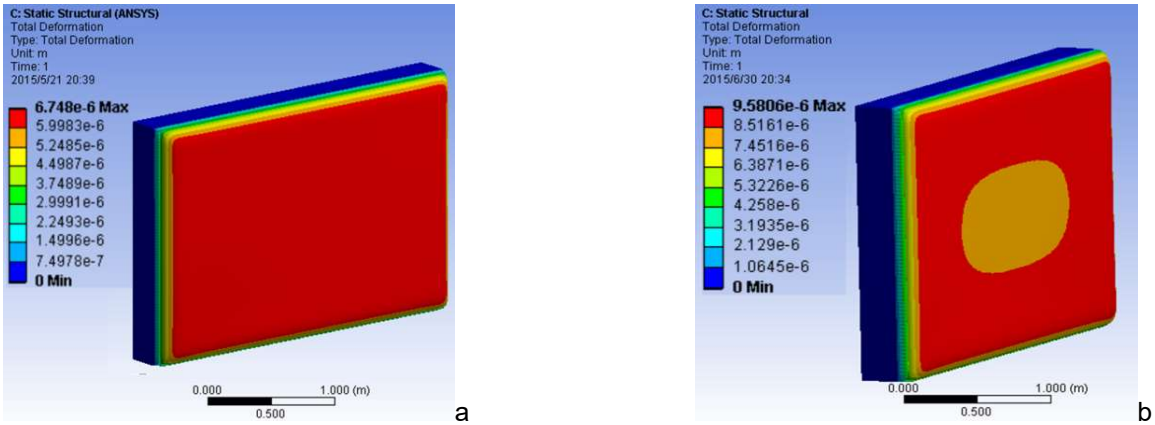

Fig.8 - Temperature deformation of WS2 as embedded slab in winter (a) and summer (b).

Because the temperature gradient and elasticity modulus of mortar and AAC layer are different, the deformation of these two layers would be inconsistent during working temperature change, which will pose a threat to the durability of wall structures, as the surface mortar layer would strip from the AAC matrix layer. Therefore, a larger deformation of surface mortar layer leads to a severer requirement for bonding strength to achieve coordinated deformation of AAC layer and mortar layer, in case of interlayer separation.

5. Conclusions

The paper presents the FEM modeling results of AAC shear walls. Simple and reliable models are established to analyze the temperature field, thermal stress and deformation of two different wall structures in winter and summer. Two mainly conclusions are drawn as follows:

(1) The insulation mortar could lower the temperature gradient within the AAC layer effectively. For AAC shear walls coated with IM, the temperature changes of AAC layers are reduced by 1.668℃ in summer and 5.315℃ in winter, compared with OM coated walls.

(2) In terms of thermal stress, mortar layers always suffer a higher stress, as the maximum in WS1 is almost doubledthan the WS2, but the maximum stress in AAC layer and interface stress of WS1 are reduced by 50%. Maximum deformation appears in AAC layer in winter but in mortar layer in summer, while deformation of AAC layer in WS1 is always smaller than that of WS2.

The simulation results reveal different properties of two AAC shear walls with ordinary or insulation mortar, which will be a guide for the selection and design of external walls in extremely cold region, taking both energy conservation and volume stability into consideration. The result from the simulation also shows that the proper use of IM may decrease the stress intension as well as the strain of outer and inner layers for self-insulation structural system.

Acknowledgement

This paper is supported by the Natural Science Foundation of China (Grant No. 51478150 & 51572251). The work is also supported by fund No.2016M591230 provided by "China Postdoctoral Science Foundation".

References

1. Q. Wang, Analysis on the technical regulation for the energy-saving reconstruction of existing residential buildings in Beijing, Architecture Technology, 2007, **38**(10), 743.
2. F. Wägner, G. Schober, and H. Mörtel, Measurement of the gas permeability of autoclaved aerated concrete in conjunction with its physical properties, Cement & Concrete Research, 1995, **25**(8), 1621.
3. I.Petrov and E. Schlegel, Application of automatic image analysis for the investigation of autoclaved aerated concrete structure, Cement & Concrete Research, 1994, **24**(5), 830.
4. K.Ramamurthy and N. Narayanan, Factors influencing the density and compressive strength of aerated concrete. Magazine of Concrete Research, 2000, **52**(3), 163.
5. K. Hanečka, O. Koronthályová and P. M. Mšovský, The carbonation of autoclaved aerated concrete, Cement & Concrete Research, 1997 **27**(4), 589.
6. J. Alexanderson, Relations between structure and mechanical properties of autoclaved aerated concrete, Cement & Concrete Research, 1979, **9**(4), 507.
7. I. Odler and M.Rößler, Investigations on the relationship between porosity, structure and strength of hydrated portland cement pastes. ii. Effect of pore structure and of degree of hydration, Cement & Concrete Research, 1985, **15**(3), 401.
8. G. C. Hoff, Porosity-strength considerations for cellular concrete, Cement & Concrete Research, 1972, **2**(1), 91.
9. S. L. Lee, R. S. Ravindrarajah, T. Y. Lim and C. T. Tam, Relationship between strength and volumetric composition of moist-cured cellular concrete, Magazine of Concrete Research, 1987, **39**(139), 115.
10. H. Ziembicka, Effect of micropore structure on cellular concrete shrinkage, Cement & Concrete Research, 1977, **7**(3), 323.
11. A. Georgiades, C. Ftikos and J. Marinos, , Effect of micropore structure on autoclaved aerated concrete shrinkage, Cement & Concrete Research, 1991, **21**(4), 655.
12. K. Ramamurthy and N. Narayanan, Influence of composition and curing on drying shrinkage of aerated concrete, Materials and Structures, 2000, **33**(4), 243.
13. J. Sun and L. Fang, Numerical simulation of concrete hollow bricks by the finite volume method, International Journal of Heat & Mass Transfer, 2009, **52**(s 23–24), 5598.
14. M. M. Al-Hazmy, Analysis of coupled natural convection–conduction effects on the heat transport through hollow building blocks, Energy & Buildings, 2006, **38**(5), 515.
15. G. Q. Du and D. H. Shi, Numerical simulation of the precast concrete box girders temperature field distribution based on material properties, Advanced Materials Research, 2013, **703**, 221.
16. A. B. Larbi, Statistical modelling of heat transfer for thermal bridges of buildings. Energy & Buildings, 2005, **37**(9), 945.
17. H. Asan, Investigation of wall's optimum insulation position from maximum time lag and minimum decrement factor point of view, Energy & Buildings, 2000, **32**(2), 197.
18. V. Kočí, J. Maděra and R. Černý, Exterior thermal insulation systems for AAC building envelopes: computational analysis aimed at increasing service life, Energy & Buildings, 2012, **47**(7), 84.
19. ANSYS, User's manual, version 14.5, ANSYS Inc., 2012.

****